

# PHYSICAL REVIEW B

## CONDENSED MATTER AND MATERIALS PHYSICS

THIRD SERIES, VOLUME 62, NUMBER 3

15 JULY 2000-I

### BRIEF REPORTS

*Brief Reports are accounts of completed research which, while meeting the usual **Physical Review B** standards of scientific quality, do not warrant regular articles. A Brief Report may be no longer than four printed pages and must be accompanied by an abstract. The same publication schedule as for regular articles is followed, and page proofs are sent to authors.*

#### Laser frequency stabilization using regenerative spectral hole burning

N. M. Strickland, P. B. Sellin, Y. Sun, J. L. Carlsten, and R. L. Cone  
*Department of Physics, Montana State University, Bozeman, Montana 59717*

(Received 5 April 2000)

We demonstrate laser frequency stabilization using a continuously regenerated *transient* spectral hole in an inhomogeneously broadened resonance of a solid. Regenerative transient holes provide extreme stabilization for time scales appropriate for spectroscopy, signal processing, ranging, and interferometry. Stabilization to 20 Hz on a 10-ms time scale using spectral holes at 793 nm in  $\text{Tm}^{3+}:\text{Y}_3\text{Al}_5\text{O}_{12}$  gives substantial improvement in the reliability of stimulated photon echoes in the same material and enables the observation of a third population storage mechanism for hole burning in  $\text{Tm}^{3+}:\text{Y}_3\text{Al}_5\text{O}_{12}$ .

Frequency stabilization of lasers is important for high-resolution spectroscopy,<sup>1</sup> applications utilizing phase-sensitive detection such as precision laser ranging, long-baseline interferometry for gravitational wave detection,<sup>2</sup> coherent optical communications, and time-domain spectral hole burning devices<sup>3</sup> for functions such as: optical signal processing<sup>4</sup> and packet switching<sup>5</sup> and radio-frequency spectrum analysis.<sup>6</sup> Modern frequency stabilization techniques use atomic or molecular resonances, such as iodine lines or laser-trapped ions<sup>7</sup> or reflection modes of high-finesse Fabry-Perot interferometers,<sup>8,9</sup> where cryogenic cavities can reduce frequency drift.<sup>10</sup> We recently reported the demonstration of a programmable frequency reference using persistent spectral hole burning<sup>11</sup> that could also be used to prepare multiple long-lived secondary frequency standards at arbitrary frequencies. Here, we demonstrate a complementary method: the use of a continuously-regenerated transient spectral hole as a viscous damping mechanism to restrict a laser's short term frequency variation—a physically different procedure from locking to a fixed atomic transition, cavity resonance, persistent spectral hole, or instantaneous samples of phase or frequency history with delayed self-heterodyne detection.<sup>12</sup>

Transient spectral holes in an inhomogeneously broadened absorption line do provide a useful reference for stabilizing a continuous-wave laser. The stability is derived from the cumulative frequency memory of the hole, lasting over the hole lifetime and potentially longer in a well-engineered closed-loop feedback system where the regenerated holes are

exact enough copies. Other frequency reference techniques can provide greater precision on long time scales, but regenerative spectral hole burning provides both vibrational immunity and excellent short term stability, which are important and sufficient requirements for many applications beyond the field of spectral hole burning (SHB). Moreover, it should be possible to engineer a system of the type we report to fit into a compact shoebox-sized apparatus that includes optics, feedback electronics, and a cryostat.

The presence of a sharp spectral hole in the inhomogeneously broadened absorption line implies a sharp dispersion in the refractive index. Pound-Drever-Hall locking<sup>8</sup> is used with a modulation frequency greatly exceeding the spectral hole resonance width to provide a feedback error signal proportional to the dispersion in the refractive index.<sup>13</sup> The unstabilized laser initially burns a jitter-broadened spectral hole, the laser frequency stabilizes to a fraction of the hole width, and the hole narrows to a limit set by the homogeneous linewidth and the laser irradiance. This self-narrowing property of regenerated holes turns hole relaxation into an advantage. The balance between spontaneous hole decay and further hole burning from continued illumination determines the equilibrium depth of the regenerating hole.

Transient spectral hole burning may be achieved by a number of storage mechanisms. The most common is population storage in the excited state of an optically active ion or molecule, providing lifetimes of up to several tens of milliseconds. Population storage in hyperfine components of the

ground state can provide far longer lifetimes, up to 20 days.<sup>14</sup> Far more systems exhibit transient SHB than exhibit persistent SHB, and this new stabilization strategy therefore gives access to a correspondingly greater range of frequencies. For the special case of SHB device applications that require a stable laser, transient spectral holes in an identical piece of the material used for the device naturally provide suitable stabilization at the needed wavelength.

We have demonstrated this stabilization technique using the  ${}^3H_6 \rightarrow {}^3H_4$  transition in  $Tm^{3+}:Y_3Al_5O_{12}$  ( $Tm^{3+}:YAG$ ) at 793 nm. The fluorescence decay time of the upper state for these samples was measured to be  $620 \mu s$  at 1.9 K, consistent with previous values.<sup>15</sup> Decay to the intermediate  ${}^3F_4$  state, with a much longer fluorescence lifetime of around 12 ms, occurs with a calculated branching ratio of 0.54 (Ref. 16) and greatly lengthens the SHB storage time of this system. We present evidence below that splittings of the  $Tm^{3+}$  ground state due to interaction with the neighboring  $Al^{3+}$  nuclear spins provide a third population storage mechanism with an even longer storage time. The potential for spectroscopy and time-domain SHB devices is illustrated by a stimulated photon echo measurement on the same transition used for locking.

We used  $Tm^{3+}:YAG$  crystals from Scientific Materials Corp. with  $Tm^{3+}$  concentrations of 0.1 at. %, giving a peak absorption coefficient of  $1.5 \text{ cm}^{-1}$  for the  ${}^3H_6(1) \rightarrow {}^3H_4(1)$  transition, and an inhomogeneous linewidth of 20 GHz. Crystal thicknesses were 5.1 and 5.3 mm for locking and 3.5 mm for photon echo measurement. The homogeneous linewidth of the transition is determined from the Mims dephasing time  $T_M$  (Ref. 17) of a two-pulse photon echo, reported as  $75 \mu s$  (Ref. 18) in the absence of an applied magnetic field. In our more dilute samples we have measured  $T_M$  to be  $116 \mu s$  (as defined in Ref. 18) and  $81 \mu s$  (with exponent  $x=2.09$  as originally defined<sup>17</sup>), corresponding to an estimated full width at half maximum homogeneous linewidth of  $\Gamma_h = 1/\pi T_M = 4 \text{ kHz}$ . The convolution of  $\Gamma_h$  during burning and reading gives a hole width of  $2\Gamma_h$  for shallow holes; deeper holes are broader due to higher absorption in the wings of the hole than at the center.

Using an apparatus described previously,<sup>11</sup> two GaAlAs external cavity diode lasers were independently frequency stabilized to transient spectral holes in separate  $Tm^{3+}:YAG$  crystals. A single cryostat held both crystals immersed in a superfluid helium bath at 1.9 K. External phase modulation at 23 and 25 MHz, respectively, produced frequency sidebands with a modulation index of 0.22. The relative stability of the two lasers was measured by heterodyne detection of unmodulated portions of the beams. Beam diameters were approximately 1 mm, with an irradiance of  $2.3 \text{ mW/cm}^2$ . A strong variation in the locking stability as the power was adjusted emphasizes the need to carefully balance the irradiance to optimize the equilibrium hole depth for locking, trading off the depth and width of the spectral hole.

Evolution of the heterodyne beat frequency is shown in Fig. 1 for cases when both lasers were free running or both locked. The inherent submegahertz free-running stabilities of these lasers are already sufficient for some spectroscopic applications but were spectacularly improved by locking each laser to a transient spectral hole. On the time scale of seconds, a clear improvement has been made, although there is

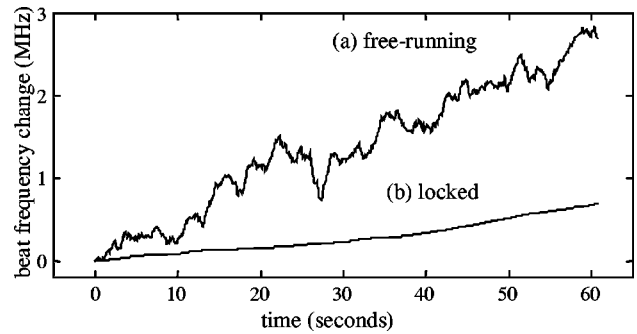


FIG. 1. Evolution of heterodyne beat signal between two lasers (a) free running, and (b) independently locked to transient spectral holes in the  ${}^3H_6 \rightarrow {}^3H_4$  transition in separate  $Tm^{3+}:YAG$  crystals.

still a drift of about 10 kHz/s in this implementation. It is on time scales faster than this that the most significant stabilization occurs, as shown by the smoothness of the curve in Fig. 1(b). A quantitative measure of frequency stability on specific time scales is provided by the two-sample or Allan variance.<sup>19</sup> The root Allan variance is shown in Fig. 2. Minimum Allan variances of 20 Hz occur for time scales of 5–10 ms, representing more than three orders of magnitude improvement in stability over the free-running lasers.

We believe that the major sources of instability are (a) residual amplitude modulation of the optical beam which causes voltage offsets upon mixing down to lower servo frequencies<sup>20</sup> and (b) thermally induced offsets and drift in the locking circuitry. These offsets corrupt the error signal and cause the laser frequency to lock slightly off the center of the hole, inducing drift as burning occurs at the shifted lock frequency. The present servo amplifier was adjusted to passively null the offset voltage at the start, but later fluctuations were uncompensated. The drift rate varied and changed directions on time scales of minutes indicating sensitivity to environmental changes. The frequency stabilization reported here was obtained without temperature stabilizing the electronics or optical setup and with vibration isolation provided by a standard pneumatically floated optical table. The current 20 Hz stabilization with an 8 kHz resonance is not limited by any material properties, nor do there appear to be fundamen-

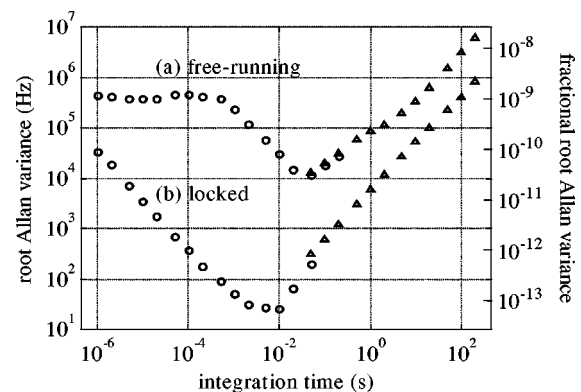


FIG. 2. Root Allan variance for the heterodyne beat frequency between two lasers (a) free running and (b) independently locked to transient spectral holes in the  ${}^3H_6 \rightarrow {}^3H_4$  transition in  $Tm^{3+}:YAG$ . Circles are measured by a frequency counter, and triangles are computed from the data of Fig. 1.

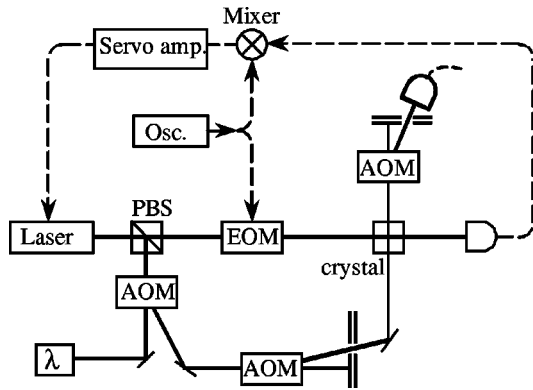


FIG. 3. Apparatus for measuring stimulated photon echoes while frequency locking to a transient spectral hole. EOM (electro-optic modulator), AOM (acousto-optic modulator), PBS (polarization beam splitter), OSC (oscillator) and  $\lambda$  wavemeter.

tal obstacles to reaching millihertz levels if the above sensitivities and offsets are reduced.

Statistically different noise sources have characteristic slopes on Allan variance plots.<sup>21</sup> Broadband phase and frequency noise (slope =  $-1$ ) limiting the left side of Fig. 2(b) may be reduced by selecting a quieter laser, a narrower spectral hole reference, or by increasing the fidelity and gain bandwidth of the servo system. Frequency drift (slope =  $+1$ ) limits the right side of Fig. 2(b) and remains the primary barrier to attaining lower variances on time scales longer than 10 ms. Reduction of external vibrational and thermal influences<sup>9</sup> may improve performance, however random frequency walks (slope =  $+0.5$ ) are not presently dominant factors on the time scales of Fig. 2.

With the high level of frequency stabilization achieved on millisecond time scales, this stabilization strategy provides ideal laser sources for optical coherent transient phenomena, in particular the photon echo and stimulated photon echo that are the basis for time-domain spectroscopy and optical devices.<sup>3-5</sup> For optimal exploitation of the stimulated photon echo, laser frequency stability is required for the storage time of the material. Since this storage time is the lifetime of a transient spectral hole for the transition being probed, the requirement is naturally met by locking to a spectral hole.

Application of this frequency stabilization strategy and its potential in optical devices was demonstrated by measuring stimulated photon echoes on the  ${}^3H_6 \rightarrow {}^3H_4$  transition of  $Tm^{3+}$ :YAG using a frequency-stabilized laser and the apparatus of Fig. 3. Approximately 1 mW of unmodulated continuous-wave power was available for producing echo excitation pulses after a portion of the laser output was phase modulated and used to frequency lock the laser to a regenerative transient spectral hole. The pulses were produced by two acousto-optic modulators, used in series to improve the on/off contrast ratio, with a third used after the crystal to block the excitation pulses. The photon echoes were detected with a thermoelectrically cooled C31034 photomultiplier. Three  $1.5 \mu s$  excitation pulses were incident on the sample, with the delay  $t_{12}$  between the first and second pulses fixed at  $6 \mu s$ . The stimulated photon echo was measured as a function of the delay  $t_{23}$  between the second and third pulses.

With the laser frequency locked to a transient spectral hole, photon echoes could be measured consistently for  $t_{23}$

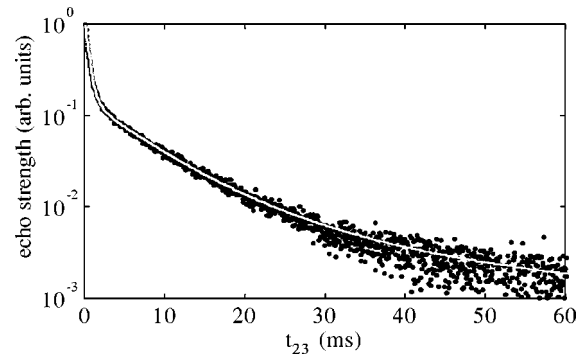


FIG. 4. Stimulated photon-echo decay on the  ${}^3H_6 \rightarrow {}^3H_4$  transition in  $Tm^{3+}$ :YAG, measured with a laser stabilized to a transient spectral hole, showing three distinct population storage mechanisms. Each point represents a single-shot event.

delay times of several tens of milliseconds, giving the data in Fig. 4. The limiting factor for measuring echoes with longer  $t_{23}$  delay times was the signal-to-noise ratio, rather than laser frequency jitter. In contrast, when the stimulated echo decay was measured with the laser free running, the reproducibility of the stimulated echo was unreliable after only  $500 \mu s$ , as shown in Fig. 5. The data points of Fig. 4 and Fig. 5 were single-shot acquisitions of the stimulated photon echo without thresholding to reject low-intensity echoes. In Fig. 5 it was clear that frequency jitter was the cause of the echo signal amplitude fluctuations, since occasionally a true-valued echo was produced when the laser frequency of the third pulse happened to match that of the first two. An envelope of true-valued echoes can be seen, but most points fall well below this. Clearly, averaging the data in Fig. 5 over multiple shots would lead to a much different and erroneous echo decay rate.

The generation of a stimulated photon echo can be considered as the scattering of the excitation pulse off the population grating generated by the first two pulses. The first two pulses create a modulation in the population of the excited state as a function of frequency, and a corresponding depletion in the ground state. The electric-field vector of the echo stimulated by the excitation pulse is proportional to the sum of these two gratings as they exist at the time of the excitation pulse. Intermediate state populations do not contribute directly to the echo but allow the ground-state depletion to remain for longer than the lifetime of the upper state. A rate

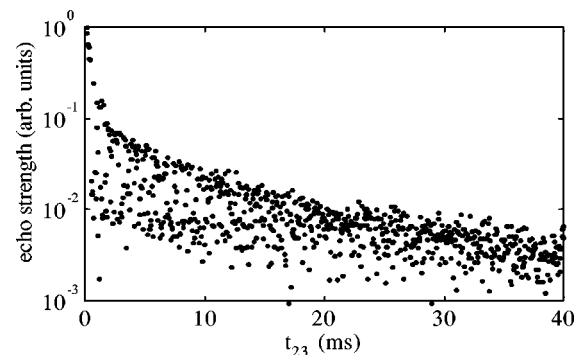


FIG. 5. Stimulated photon-echo decay on the  ${}^3H_6 \rightarrow {}^3H_4$  transition of  $Tm^{3+}$ :YAG, without frequency stabilization of the laser. Each point represents a single-shot event.

equation analysis for a four-level system shows that the echo electric field decays with increasing  $t_{23}$  delay time as the sum of three exponential functions whose decay times are the lifetimes of the three excited states involved. The detected echo strength is the square of this function.

The square root of the echo intensity was fitted to three exponentials giving the solid white line in Fig. 4 with decay times of 590  $\mu$ s, 11.8 ms, and 90 ms. The first decay time corresponds to population storage in the  $^3H_4$  excited state of the transition, in agreement with the 620  $\mu$ s value obtained from fluorescence decay. The second corresponds to population storage in the intermediate  $^3F_4$  metastable state, a mechanism previously shown to account for transient spectral hole burning in  $Tm^{3+}$  doped crystals.<sup>22</sup> The third, longest decay component has an uncertainty of about 50% for its decay time due to the scatter of the data attributed to detector noise. This component is assigned to an energy shift arising from the coupling of  $Tm^{3+}$  to the nuclear spins of lattice  $Al^{3+}$  ions. To confirm the nuclear-spin coupling contribution to the population storage, the stimulated echo decay was re-

measured with a permanent magnet placed immediately beneath the cryostat. This produced a very modest magnetic field at the crystal ( $\sim 100$ G), but it was enough to show a distinct increase of the decay time associated with this level structure, corresponding to increased spin-lattice relaxation times.

In conclusion, regenerative transient spectral hole burning can provide an effective means for stabilizing the frequency of a laser. A high degree of stabilization can be achieved, as the spectral holes in some materials can be narrower than 100 Hz. This stabilization method is well suited for spectroscopy and for optical data processing devices based on time-domain spectral hole burning since separate pieces of the same material can be used as stabilizer and processor. A substantial improvement in stimulated photon-echo reproducibility was demonstrated.

We thank J. L. Hall and W. R. Babbitt for helpful discussions. This research was supported by the U.S. Air Force Office of Scientific Research, Grant No. F49620-96-1-0466.

- 
- <sup>1</sup>R.G. DeVoe and R.G. Brewer, Phys. Rev. Lett. **50**, 1269 (1983); M.J. Sellars, R.S. Meltzer, P.T.H. Fisk, and N.B. Manson, J. Opt. Soc. Am. B **11**, 1468 (1994).
- <sup>2</sup>A. Abramovici *et al.*, Phys. Lett. A **218**, 157 (1996); K. Danzmann, Class. Quantum Grav. **14**, 1399 (1997).
- <sup>3</sup>T.W. Mossberg, Opt. Lett. **7**, 77 (1982); A. Rebane, R. Kaarli, P. Saari, A. Anijalg, and K. Timpmann, Opt. Commun. **47**, 173 (1983); M. Mitsunaga, R. Yano, and N. Uesugi, Opt. Lett. **16**, 1890 (1991); M. Mitsunaga, N. Uesugi, H. Sasaki, and K. Karaki, *ibid.* **19**, 752 (1994); H. Lin, T. Wang, and T.W. Mossberg, *ibid.* **20**, 1658 (1995).
- <sup>4</sup>N.W. Carlson, L.J. Rothberg, A.G. Yodh, W.R. Babbitt, and T.W. Mossberg, Opt. Lett. **8**, 483 (1983); M. Zhu, W.R. Babbitt, and C.M. Jefferson, *ibid.* **20**, 2514 (1995); K.D. Merkel and W.R. Babbitt, *ibid.* **24**, 172 (1999).
- <sup>5</sup>X.A. Shen and R. Kachru, Opt. Lett. **20**, 2508 (1995); T. Wang, H. Lin, and T.W. Mossberg, *ibid.* **20**, 2541 (1995); T.L. Harris, Y. Sun, R.L. Cone, R.M. Macfarlane, and R.W. Equall, *ibid.* **23**, 636 (1998).
- <sup>6</sup>J.-P. Galaup, F. Grelet, J.-L. Le Gouet, D. Dolfi, and J.-P. Huignard, *Analyseur de Spectre de Frequence*, French Patent, INPI Registration No: FR9802626, registration date: March 4, 1998, INPI Publication No.: FR2775790, date of publication: September 9, 1999.
- <sup>7</sup>D.J. Berkeland, J.D. Miller, J.C. Bergquist, W.M. Itano, and D.J. Wineland, Phys. Rev. Lett. **80**, 2089 (1998).
- <sup>8</sup>R.W.P. Drever, J.L. Hall, F.V. Kowalski, J. Hough, G.M. Ford, A.J. Munley, and H. Ward, Appl. Phys. B: Photophys. Laser Chem. **31**, 97 (1983); M. Zhu and J.L. Hall, J. Opt. Soc. Am. B **10**, 802 (1993).
- <sup>9</sup>B.C. Young, F.C. Cruz, W.M. Itano, and J.C. Bergquist, Phys. Rev. Lett. **82**, 3799 (1999).
- <sup>10</sup>S. Seel, R. Storz, G. Ruoso, J. Mlynek, and S. Schiller, Phys. Rev. Lett. **78**, 4741 (1997).
- <sup>11</sup>P.B. Sellin, N.M. Strickland, J.L. Carlsten, and R.L. Cone, Opt. Lett. **24**, 1038 (1999); N.M. Strickland, R.L. Cone, and R.M. Macfarlane, Phys. Rev. B **59**, 14 328 (1999).
- <sup>12</sup>Y.T. Chen, Appl. Opt. **28**, 2017 (1989); J. L. Hall, *Method and Apparatus for Laser Control*, Patent No. 4,856,009, August 8, 1989; C. Greiner, B. Boggs, T. Wang, and T. Mossberg, Opt. Lett. **23**, 1280 (1998).
- <sup>13</sup>G.C. Bjorklund, M.D. Levenson, W. Lenth, and C. Ortiz, Appl. Phys. B: Photophys. Laser Chem. **32**, 145 (1983); J.M. Supplee, E.A. Whittaker, and W. Lenth, Appl. Opt. **33**, 6294 (1994).
- <sup>14</sup>W.R. Babbitt, A. Lezama, and T.W. Mossberg, Phys. Rev. B **39**, 1987 (1989); F.L. Könz, Y. Sun, R.L. Cone, R.W. Equall, and R.M. Macfarlane (unpublished).
- <sup>15</sup>G. Armagan, A.M. Buoncristiani, and B. DiBartolo, Opt. Mater. **1**, 11 (1992).
- <sup>16</sup>J.A. Caird, L.G. DeShazer, and J. Nella, IEEE J. Quantum Electron. **QE-11**, 874 (1975).
- <sup>17</sup>W.B. Mims, Phys. Rev. **168**, 370 (1968).
- <sup>18</sup>R.M. Macfarlane, Opt. Lett. **18**, 1958 (1993).
- <sup>19</sup>D.W. Allan, IEEE Trans. **UFFC-34**, 647 (1987).
- <sup>20</sup>N.C. Wong and J.L. Hall, J. Opt. Soc. Am. B **2**, 1527 (1985); F.L. Walls, IEEE Trans. **UFFC-34**, 592 (1987); R. W. Fox, L. D'Evelyn, H. G. Robinson, C. S. Weimer, and L. Hollberg, Proc. SPIE **2378**, 58 (1995).
- <sup>21</sup>J. Rutman, Proc. IEEE **66**, 1048 (1978).
- <sup>22</sup>R.M. Macfarlane, Opt. Lett. **18**, 829 (1993).